

Exploring the feasibility of lossy compression for PDE simulations

Jon Calhoun¹, Franck Cappello², Luke N Olson³,
Marc Snir³ and William D Gropp³

The International Journal of High
Performance Computing Applications
2019, Vol. 33(2) 397–410

© The Author(s) 2018

Article reuse guidelines:

sagepub.com/journals-permissions

DOI: 10.1177/1094342018762036

journals.sagepub.com/home/hpc



Abstract

Checkpoint restart plays an important role in high-performance computing (HPC) applications, allowing simulation runtime to extend beyond a single job allocation and facilitating recovery from hardware failure. Yet, as machines grow in size and in complexity, traditional approaches to checkpoint restart are becoming prohibitive. Current methods store a subset of the application's state and exploit the memory hierarchy in the machine. However, as the energy cost of data movement continues to dominate, further reductions in checkpoint size are needed. Lossy compression, which can significantly reduce checkpoint sizes, offers a potential to reduce computational cost in checkpoint restart. This article investigates the use of numerical properties of partial differential equation (PDE) simulations, such as bounds on the truncation error, to evaluate the feasibility of using lossy compression in checkpointing PDE simulations. Restart from a checkpoint with lossy compression is considered for a fail-stop error in two time-dependent HPC application codes: PlasComCM and Nek5000. Results show that error in application variables due to a restart from a lossy compressed checkpoint can be masked by the numerical error in the discretization, leading to increased efficiency in checkpoint restart without influencing overall accuracy in the simulation.

Keywords

Lossy compression, checkpoint restart, exascale, error tolerance selection, error propagation, fault tolerance, compression

1. Introduction

High-performance computing (HPC) applications rely on checkpoint restart to extend execution time beyond the requested allocation time and to tolerate failures in software and in hardware during the simulation run. While the performance and memory of HPC systems continue to increase in size, one potential bottleneck in continued use of checkpoint restart is that file system bandwidth has exhibited only slow growth in current machines. For example, the current 10 petaflop machines Blue Waters at the University of Illinois and Titan at Oak Ridge National Laboratory and the upcoming 100 petaflop machine Sierra¹ at Lawrence Livermore National Laboratory, all incorporate 1 TB/s file systems. The new machine Summit² at Oak Ridge National Laboratory increases the file system bandwidth to 2.5 TB/s. However, since the memory capacity in the 100 petaflop systems is approximately 5–9 times larger than in current 10 petaflop systems, scalable applications are expected to see an increase in checkpoint restart times with a similar factor. However, as HPC systems continue to increase in size and complexity, new design constraints (Bergman et al., 2008; Shalf et al., 2010) such as the high

cost of data movement and comparatively free cost of computation allow for new optimizations.

Exascale systems are expected to put further pressure on the checkpoint system as the mean time between failure (MTBF) is expected to decrease, thus demanding more frequent checkpointing (Cappello et al., 2009). This aspect has motivated so-called multi-level checkpoint restart (Bautista-Gomez et al., 2011; Moody et al., 2010) schemes, where the memory hierarchy is leveraged to reduce the time to checkpoint and to recover when a failure occurs. The addition of burst buffers (Liu et al., 2012) to HPC

¹ Holcombe Department of Electrical and Computer Engineering, Clemson University, Clemson, SC, USA

² Mathematics and Computer Science Division, Argonne National Laboratory, Lemont, IL, USA

³ Department of Computer Science, University of Illinois at Urbana-Champaign, Urbana, IL, USA

Corresponding author:

Jon Calhoun, Holcombe Department of Electrical and Computer Engineering, Clemson University, 433 Calhoun Dr, 104 Riggs Hall, Clemson, SC 29634, USA.

Email: calhou3@clemson.edu

systems offers another approach to reduce time to checkpoint. Yet, multi-level checkpointing and burst buffers do not target a reduction in checkpoint size, which is another major avenue for checkpoint time reduction. Compression of the state variables can be used to reduce the checkpoint size. The relative cost of compression decreases as computation becomes cheaper relative to the cost of data movement. For example, for processors on HPC systems, a single IEEE-754 fused multiply-add consumes three orders of magnitude less energy than a dynamic random-access memory (DRAM) memory operation (Sardashti, 2015). In addition, the cost of data movement increases as the memory hierarchy is traversed from registers to file systems.

Standard compression techniques are often ill-suited for floating-point data (Son et al., 2014) which has prompted the development of floating-point-specific compressors. These are often lossless algorithms (Burtscher and Ratana-worabhan, 2007; Lindstrom and Isenburg, 2006) and, in most cases, achieve around a 50% reduction in checkpoint size. By switching to lossy compression schemes (Di and Cappello, 2016; Lakshminarasimhan et al., 2011; Lindstrom, 2014), higher compression ratios are achieved.

Previous works (Laney et al., 2013; Ni et al., 2014; Sasaki et al., 2015) have shown success in restarting from a lossy checkpoint but have not focused on the relationship between the compression error and the truncation error of the numerical approximations used in the simulation. Establishing this relation is fundamental to guaranteeing correctness for users of numerical simulations.

Various break-even points for system and application level checkpointing have been analyzed for lossless compressors on HPC machines (Ibtessham et al., 2012). For lossy compression, the performance benefits are realized if the overall checkpoint time is reduced. Thus, the time to compress plays a key role in analysis. Lossy compression often exhibits improved compression and decompression times in comparison to lossless schemes (Di and Cappello, 2016; Lakshminarasimhan et al., 2011).

This article investigates the feasibility of using lossy compression for checkpointing PDE simulations, by interpreting the error introduced through lossy compression as numerical error and by relating it to spatial discretization error and approximation properties in the numerical methods used in simulation. The article highlights two important PDE model problems (advection and diffusion) and two production-level HPC applications (PlasComCM³ and Nek5000⁴) and shows that the error introduced by lossy compression at restart does not increase beyond the discretization error, even in the scenario of multiple restarts in the same execution. This underscores the idea that the compression error exhibits little influence on the quality of the final result of the simulation.

Specifically, the contributions are

- expression of lossy compression error as numerical error;
- the relationship between error due to lossy compression with physical properties in the problem;

- a discussion of boundary conditions and the attenuation of compression error;
- the feasibility of lossy compression for checkpoint-restart on kernels and real applications; and
- a performance model that distinguishes the trade-off between efficiency and accuracy in lossy compression.

The rest of this article is outlined as follows. Section 2 discusses related work in the area of compression and HPC checkpoint restart. Section 3 outlines the relationship between error introduced through lossy compression and the approximation properties of the discretization. Section 4 uses approximation bounds to investigate propagation and reduction of error through two model PDE problems. Section 5 gives an overview of two production-level applications, PlasComCM and Nek5000, and presents results from using a compression tolerance that is consistent with the numerical properties of the simulation. Section 6 uses a performance model to explore efficiency of lossy compression. Section 7 presents a discussion of new research directions based on this work. Finally, we conclude in Section 8.

2. Related work

The applicability of lossy compression for data transfer to and from main memory has been studied for several applications, including LULESH, pF3D, and Miranda (Laney et al., 2013), where simulation correctness is measured by post-simulation analysis of the physics. In this article, we utilize the application's spatial discretization properties to construct a bound for the amount of error allowed in the simulation. The benefit is that the accuracy of the associated numerical method is known a priori and compression error can be dominated by the discretization truncation error. Another approach uses a two-stage scheme to compress: first lossy, then lossless (Ni et al., 2014). The checkpoint size is observed to be around 15% of the original size and restarts are shown to be successful. Another observation is that errors introduced through a particular variable may result in a large propagation of error, leading to the use of lossy compression on only a subset of the checkpointed variables. Wavelet-based lossy compression has been used in the Non-hydrostatic Icosahedral Atmospheric Model (NICAM) climate application (Sasaki et al., 2015), where it is shown that the relative error remains less than 1.5% 1500 time-steps after restart from a lossy compressed checkpoint. One disadvantage is that the error continues to grow linearly with time. An evaluation of lossy compression on the community earth system model data sets (Baker et al., 2014) uses metrics such as max-norm, normalized root-mean-square error, and Pearson's correlation coefficient to characterize how the data set changes due to compression error. However, this work does not consider restarting a simulation from a lossy compressed checkpoint. This article complements (Baker et al., 2014) by providing and evaluating a methodology of selecting lossy compression error bounds that allow

simulations to be successfully restarted from lossy compressed checkpoints.

A critical characteristic of lossy compression is the *level* of lossy compression—that is, compression factor (factor by which the data set size is reduced). Compression factors are dependent on the magnitude of error that the compressor introduces. Higher compression factors lead to larger errors, but the magnitude of acceptable compression error is problem dependent. A natural approach to determine the acceptability of a compression error is to compare the lossy state with that of an uncompressed checkpoint and verify it passes simulation validation metrics. This trial and error method can be effective; however, a more direct route is to compare the compression error to the approximation properties in the application. This article explores the applicability of lossy compressed checkpointing from the numerical perspective and provides guidance on the setting of the lossy compressed checkpointing compression error tolerance.

Control of compression error is an important trait of a compressor. Indeed, only a strict control of the compression error allows for the association between lossy compression and the properties of the numerical methods. Lossy compressors for floating-point data sets, such as ISABELA (Lakshminarasimhan et al., 2011), NUMARCK (Chen et al., 2014), ZFP (Lindstrom, 2014), FPZIP (Lindstrom and Isenburg, 2006), and SZ (Di and Cappello, 2016; Tao et al., 2017), allow for varying degrees of control. In this work, SZ is used since the compressor adheres to prescribed relative and absolute bounds on the tolerance on a per element basis and provides the highest compression factors. In particular, SZ-1.3 is used, although other compressors fit within the scope of this work.

3. Linking compression error to numerical error

3.1. Lossy compressor SZ

To use SZ, the user sets the error bound by selecting the tolerance, ϵ . It is chosen so that the difference between the original values and decompressed values is bounded relatively and/or absolutely by ϵ .

SZ compresses data by predicting value $i + 1$ from values at i , $i - 1$, and $i - 2$ using curve fitting (constant, linear, or quadratic). If the value predicted is within the prescribed tolerance, then the curve fitting function predicting $i + 1$ is encoded as a codeword indicating the curve fitting method used. If the value at $i + 1$ is inaccurate using a curve fitting, then an escaped codeword is encoded. The value of $i + 1$ is then added to a list of other hard-to-compress data values. This list is compressed by inspecting the binary representations of the data for commonality. For multi-dimensional data, SZ explores prediction in all spatial dimensions when curve fitting. SZ has compression routines for single and double precision arrays. This article uses the double precision compression routines during all experiments because

all model problems and test applications use double precision for their main computation.

3.2. Method

Selecting the correct level of lossy compression is often based on trial and error. The quality of a decompressed checkpoint is ultimately application dependent and assessing the quality requires deep knowledge of the underlying physics. To this end, a priori bounds on the numerical discretization scheme are useful in quantifying error in specific variables of the simulation. In addition, numerical stability of the numerical method plays an important role.

This article exploits the fact that many HPC applications approximate the solution to PDEs or ordinary differential equations (ODEs). The level of accuracy given by the truncation error gives us an upper bound on compression error tolerances. A compression tolerance less than the truncation error produces results that are within a factor of the discretization error, but not bit-reproducible to the uncompressed solution. A compression tolerance greater than truncation error will add more error into the state variables, potentially impacting simulation results.

To understand truncation error, consider an approximation of $u(x + h)$ by Taylor series expansion, a method used in deriving and analyzing numerical methods to solve PDEs and ODEs:

$$u(x + h) = u(x) + u'(x)h + \frac{u''(x)h^2}{2} + \mathcal{O}(h^3) \quad (1)$$

This Taylor series truncates $u(x + h)$ to second-order accuracy. Therefore, any error that is less than $\mathcal{O}(h^2)$ results in a numerically equivalent approximation to $u(x + h)$ according to the accuracy specified when truncating the Taylor series.

The approach used in this article is to select a level of lossy compression that results in an error that is less than the spatial discretization error of the problem. A similar approach to ours is presented in Fischer et al. (2017) and uses estimates on simulation accuracy to reduce the communication volume in parallel ODE solvers by compressing floating-point values via truncation. In addition, Fischer et al. (2017) prove the stability and convergence of their numerical scheme with the introduced, controlled perturbations during communication. In this article, we computationally verify our methodology for selecting lossy compression error tolerances. Future work will evaluate our methodology theoretically. Given a spatial mesh size, h_x in 1-D, the order of accuracy of the method is specified as $\mathcal{O}(h_x^p)$, where p is the order of discretization accuracy. A simulation that uses a second-order discretization with $h_x = 0.1$ suggests an error of approximately $e \approx ch_x^2 = c \cdot 0.01$, for some constant c .⁵ This implies that a numerical approximation, u^h , and a perturbed numerical approximation $\tilde{u}^h = u^h + \epsilon$ are close if $\epsilon < \mathcal{O}(h_x^2)$. This motivates the approach taken in this article, where the compression tolerance ϵ is selected such that it is less than the simulation's

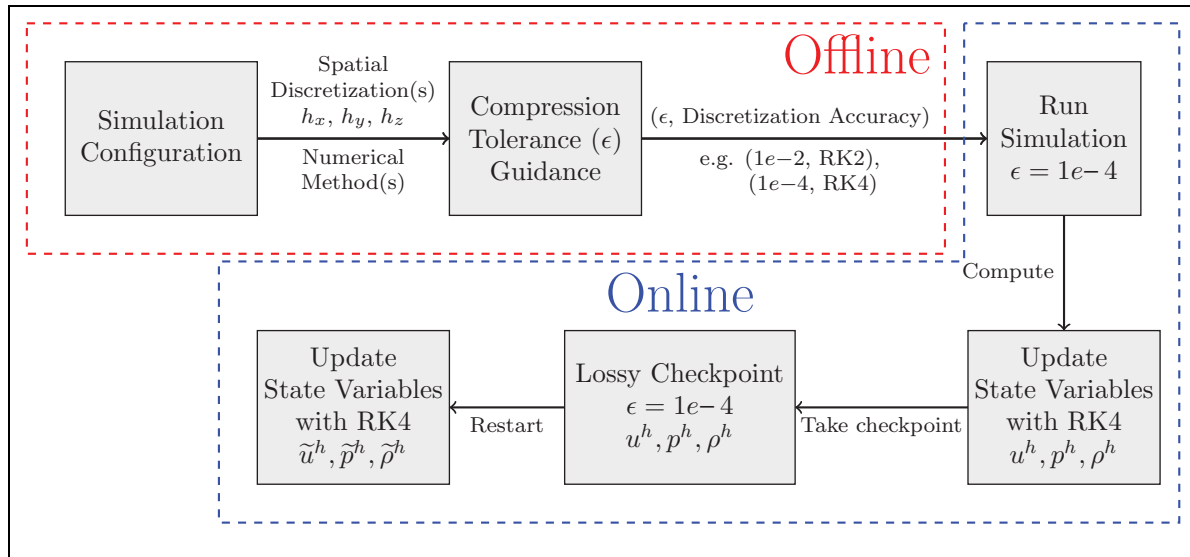


Figure 1. Overview of method to select the lossy compression error tolerance using a Runge-Kutta numerical method.

truncation error e^h .⁶ Adding compression error less than e^h creates a perturbed numerical approximation \tilde{u}^h equivalent to u^h based on the level of approximation in u^h . For problems that use adaptive mesh refinement, the compression tolerance is selected dynamically just before the application is checkpointed based on the current finest grid resolution and is the study of future work.

Figure 1 details the selection of lossy compression error tolerances. The numerical accuracy and spatial discretization size are used to calculate a bound on the error and to produce a compatible compression error tolerance. Optionally, the error tolerance can be further refined by leveraging application-specific knowledge about the problem such as convergence properties, physical domain, and boundary conditions. After restart from a lossy compressed checkpoint, results are not bit-reproducible to those from the standard approach but are within the simulation's numerical accuracy.

Our method can also be used to guide the selection of tolerances to allow more error in return for higher compression factors. For example, if ϵ is the compression tolerance for a fourth-order accurate method, it is straightforward to identify a compression tolerance, γ for a second-order method. This new tolerance γ allows for higher compression factors at the expense of larger errors in the data. Data compressed with the new tolerance γ can be interpreted as a low-order approximation to the original data. In fact, similar approaches are used in HPC applications such as Nek5000 to reduce checkpoint size. On restart, Nek5000 bootstraps itself with a low-order method which may only require information from the previous time-step. Once the program has iterated enough through time with the low-order method that a high-order method is valid, the application switches to the high-order method for the remainder of the simulation.

Algorithm 1 outlines a generic time-stepping code that utilizes lossy compression during checkpoint restart. The

Algorithm 1. Outline of generic time-stepping code that uses lossy compressed checkpoints.

Input: e^h : User estimate of truncation error.
 ϵ : User selected compression error tolerance less than e^h .
 checkpoint_interval: Number of iterations between checkpoints.

```

1 Function main()
2   if restarting == FALSE then
3      $u \leftarrow \text{initVelocity}()$ 
4      $p \leftarrow \text{initPressure}()$ 
5      $\rho \leftarrow \text{initDensity}()$ 
6   else
7      $u \leftarrow \text{readDecompressVelocity}()$ 
8      $p \leftarrow \text{readDecompressPressure}()$ 
9      $\rho \leftarrow \text{readDecompressDensity}()$ 
10  for  $t \leftarrow 0$  to  $T$  do
11     $u \leftarrow \text{updateVelocity}()$ 
12     $p \leftarrow \text{updatePressure}()$ 
13     $\rho \leftarrow \text{updateDensity}()$ 
14    if  $t \bmod \text{checkpoint\_interval} == 0$  then
15      lossyCompressCheckpoint( $u, p, \rho, \epsilon$ )

```

user computes an a priori bound on the simulation's truncation error e^h by using the smallest spatial mesh size and the numerical method's order of accuracy as outlined above. Next, the user selects a compression error tolerance, ϵ , less than the truncation error, e^h . The simulation starts and runs as normal until a checkpoint is taken. The state variables u , p , and ρ represent the physical properties velocity, pressure, and density, respectively. These physical properties are fundamental to computational fluid dynamics codes such as PlasComCM and Nek5000. As the simulation progresses, the state variables u , p , and ρ are lossy compressed

before the checkpoint is written. After the checkpoint is established, computation proceeds as normal until the final time-step. If the simulation requires a restart before reaching the final time-step, then the lossy checkpoint is read and computation proceeds using the decompressed versions of the state variables.

4. Understanding compression error behavior on 1-D model problems

To motivate the approach outlined in Section 3, two model PDEs are presented: 1-D heat and 1-D advection equations. These two model PDEs are selected to highlight the impact of physical properties on the selection of lossy compression error tolerances. The behavior of these model problems is reflected in more complex HPC applications, as observed in Section 5.

4.1. 1-D heat

The 1-D heat equation finds the temperature solution $u(x, t)$ for all positions x and time t along a rod with fixed length L is given by

$$u_t = u_{xx} + q(x), \quad 0 < x < 1, \quad (2)$$

$$u(0, t) = 20, u(L, t) = 50, \quad t > 0 \quad (3)$$

$$u(x, 0) = f(x), \quad 0 < x < L, \quad (4)$$

where $q(x)$ is a time-independent external heat source forcing term along the length of the rod. For this example, Backward Euler with second-order finite differences is used to discretize equation (2) yielding

$$\frac{u_j^{n+1} - u_j^n}{h_t} - \frac{u_{j+1}^{n+1} - 2u_j^{n+1} + u_{j-1}^{n+1}}{h_x^2} = q(x). \quad (5)$$

This results in a tri-diagonal linear system that is solved using a direct method at each time-step to simulate the PDE. The numerical accuracy of equation (5) is $\mathcal{O}(h_t; h_x^2)$, first-order accurate in time and second-order accurate in space. Thus, errors in the solution that are much smaller than $\mathcal{O}(h_t; h_x^2)$ will not impact the overall accuracy of the numerical approximation. Since restarting from a lossy compressed checkpoint adds an error into the simulation, this lossy compression error tolerance is selected so that the error is below the truncation error of the numerical scheme. For this problem, $h_x = 0.02$ implies an accuracy of $e^h = 0.02^2 = 4e-4$ and a compression tolerance of $\epsilon = 1e-4$. Figure 2 shows error in the solution of equation (5) with and external heat source:

$$q(x) = \begin{cases} 100 & : x = L/2 \\ 0 & : x \neq L/2 \end{cases}$$

Figure 2 shows the error $e = u^h - \tilde{u}^h$ in restarting the simulation at time $t = 0.6$ and $t = 1.1$ from lossy compressed checkpoints at the preceding time steps of $t = 0.5$

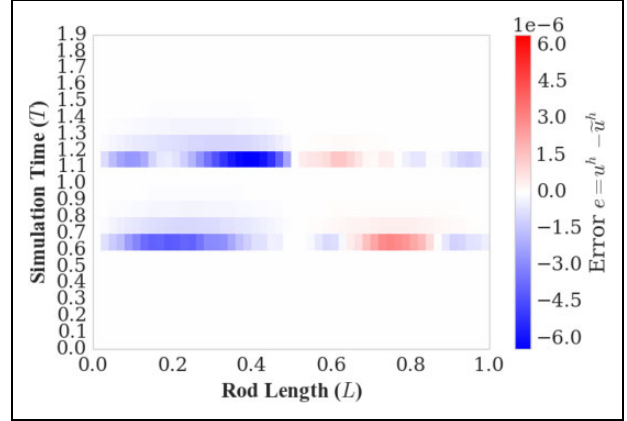


Figure 2. Error at each grid-point in a 1-D heat equation between numerical solution, u^h , and a numerical solution restarted from lossy checkpoints, \tilde{u}^h , at time $t = 0.6, 1.1$.

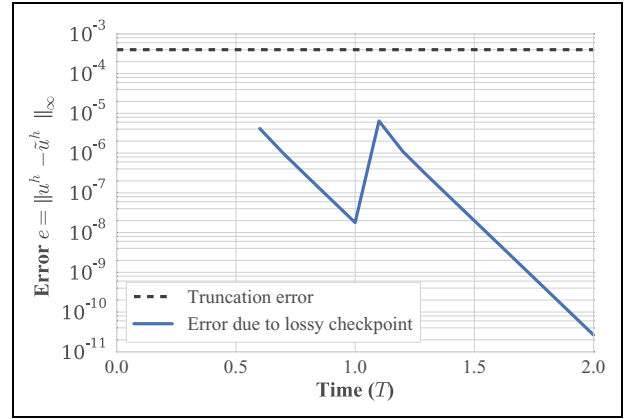


Figure 3. Maximum absolute error in the compressed numerical solution, \tilde{u}^h due to restarting from a lossy compressed checkpoint for 1-D heat equation (2).

and $t = 1.0$, respectively. Each tick on the y-axis section represents a single time-step in the simulation. The state of the second restart is affected by two lossy compressed checkpoints. A blank (white) region in the figure denotes no error in the compressed numerical solution, \tilde{u}^h , compared to an uncompressed numerical solution u^h . After restart, Figure 2 shows that error is distributed throughout the entire domain and is attenuated after a few time-steps. This is expected as this PDE models heat conduction, resulting in smooth solutions and propagation of error through the domain as time advances. In addition, with the selection of a constant temperature boundary condition, the solution converges to a steady-state solution. This property further accelerates the aforementioned removal of error in the heat equation.

Figure 3 underscores the limited impact of lossy compression at a tolerance of $\epsilon = 1e-4$, which does not contribute to error above the truncation error of $e^h = 4e-4$. Thus, the numerical solution that depends on two restarts from lossy compressed checkpoints, \tilde{u}^h , is equivalent to the original numerical solution, u^h . Although the solution is

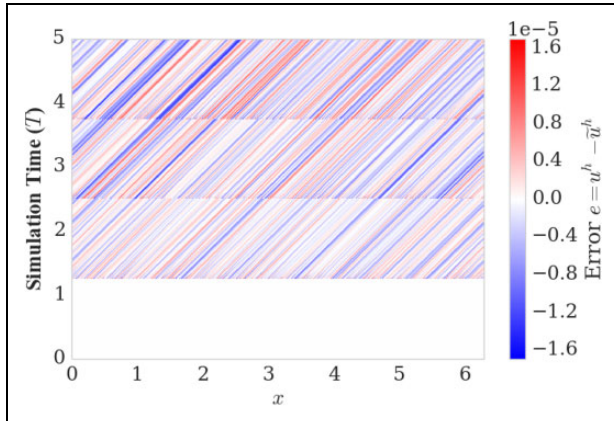


Figure 4. Error at each grid-point in a 1-D advection equation between a normal numerical solution, u^h , and a numerical solution restarted from lossy checkpoints, \tilde{u}^h , at times $t = 1.25, 2.5$, and 3.75 .

compressed to a tolerance $\epsilon = 1e-4$, the resulting error in \tilde{u}^h is small due to the smoothness of the solution between any two consecutive points in the domain being easily predicted by the lossy compressor.

4.2. 1-D advection

A notable aspect of the heat equation (2) is the attenuation of error as time evolves. The advection equation (6) does not have such a property. Instead, solutions (and error) propagate following a characteristic in the direction of flow. Any corruption in the solution remains in the wave until it reaches the boundary of the domain. In contrast, application of periodic boundaries does not allow error to escape the domain. As a result, error accumulates with each restart from a lossy compressed checkpoint. To illustrate this point, consider a 1-D advection equation with periodic boundaries:

$$\begin{aligned} u_t &= -u_x, \quad 0 < x < 2\pi \\ u(0, t) &= u(L, t), \quad t > 0 \\ u(x, 0) &= f(x), \quad 0 < x < L \end{aligned} \quad (6)$$

The equations in (6) are solved using Lax–Wendroff, which has a spatial truncation error of $\mathcal{O}(h_x^2)$, and with an initial condition of $u(x, 0) = f(x) = \sin(3x)$. In this example, the lossy compression error tolerance is set at $\epsilon = 1e-5$ since the spatial discretization of $h_x = 0.006$ suggests accuracy up to $0.006^2 = 3.6e-5 = e^h$. The restarts occur at times $t = 1.25, 2.5$, and 3.75 . In Figure 4, the error history shows that with each successive restart, the error persists (error lines do not reduce in magnitude between checkpoints), increases (error lines become darker with the number of checkpoints), and is propagated through the domain in the direction of advection (error at each point shifts to the right as time increases). If periodic boundary conditions are not used, then error still exists between the two solutions due to the restart, but only until the component of the error leaves the domain.

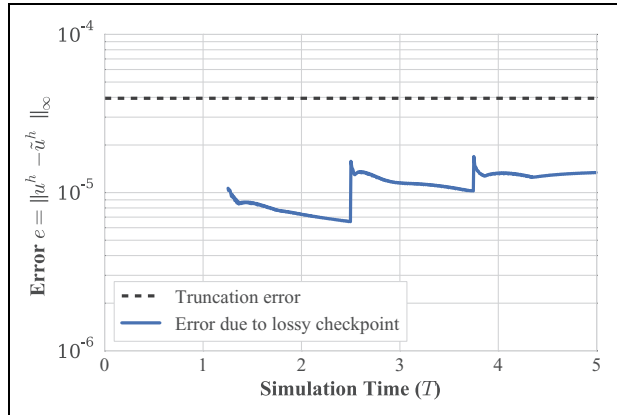


Figure 5. Maximum absolute error in a compressed numerical solution, \tilde{u}^h , due to restarting from lossy compressed checkpoints for 1-D advection equation (6). Restarts from a lossy checkpoint occur at times $t = 1.25, 2.5$, and 3.75 .

Periodic boundary conditions allow for the accumulation of error shown in Figure 5. Figure 5 shows that the maximum error in the compressed numerical solution \tilde{u}^h at each time-step is always less than truncation error for this simulation, even when restarting multiple times. The compression error tolerance is chosen to guarantee this by staying below the truncation error of the method. This is done heuristically in a small training run by observing the max-norm over the first few time-steps after restarting and selecting a tolerance, ϵ , that yields a max-norm roughly an order of magnitude less than the truncation error, e^h , to allow for unforeseen accumulation. This can be repeated in quick succession to gauge the impact of multiple restarts.

5. Lossy compressing production applications

This section applies the approach of selecting lossy compression error tolerances from Section 3 to two production-level HPC applications: PlasComCM and Nek5000. Results are collected on Blue Waters, a Cray machine managed by the National Center for Supercomputing Applications. This article uses the XE6 nodes on the machine, which are equipped with 64 GB of memory and two AMD Interlagos CPUs per node. The checkpointing routines of PlasComCM and Nek5000 are modified to lossy compress all state variables just before they are written to disk. Each state variable is compressed with SZ-1.3 (Di and Cappello, 2016) using relative and absolute error bounds. In production runs of both applications, checkpoints are taken every 1000–3000 time-steps which equates to around 1–10% of simulation time for the data sets used during testing. Simulations with a higher percentage of execution time devoted to I/O exhibit a larger portion of time spent in checkpointing.

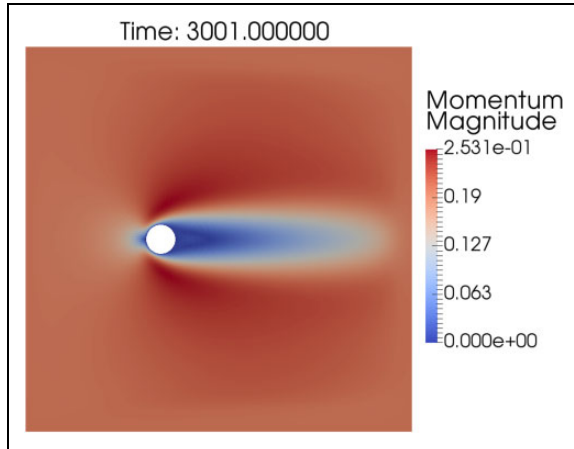


Figure 6. Momentum magnitude after 60,020 time-steps for PlasComCM. The fixed cylinder object (white circle) obstructs the flow causing momentum to slow around the object in the direction of flow (to the right).

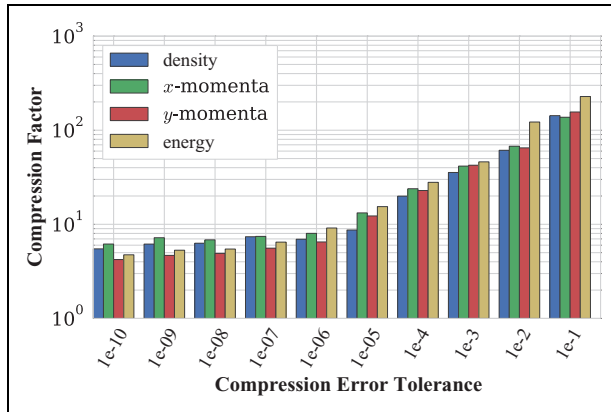


Figure 7. Compression factors for PlasComCM.

5.1. PlasComCM

The first example uses PlasComCM,⁷ a multi-physics plasma combustion code. The core functionality of the code targets the incompressible Navier–Stokes equations. Production runs checkpoint 1 MB–1 GB per process. Here, the 2-D homogeneous Euler equations are used as a model problem. Inside the domain, there is a fixed cylindrical object obstructing the flow (Figure 6). An overset mesh is placed around the cylinder to help resolve the obstructed flow. This problem is run with four processes, each checkpointing about 1 MB of data per process in an HDF5 file using an application-specific checkpointing routine. The momentum solution of this problem after evolving for 60,020 time-steps is shown in Figure 6.

The checkpoint file in PlasComCM consists of four state variables: density, x -momenta, y -momenta, and energy. Figure 7 shows a large difference in the compression factor depending on the selected compression error tolerance ranging from $104\times$ for $\epsilon = 1e-1$ to $2.2\times$ for $\epsilon = 1e-10$. Compression factors for small error tolerances are consistent with

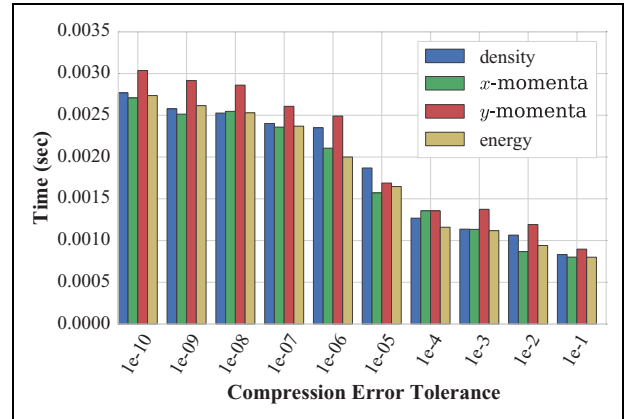


Figure 8. Compression time for PlasComCM (per process, single threaded).

reported lossless compression factors (Son et al., 2014). As the compression error tolerances decrease, there is a corresponding increase in compression time as shown in Figure 8. Compressing with small error tolerances results in SZ’s curve fitting methods not being able to accurately predict the values within the specified error tolerance. This forces SZ to compress these values using binary inspection. This second pass increases compression time and does not yield as significant of a reduction as curve fitting and encoding.

The 2-D flow problem is solved using fourth-order Runge–Kutta with $h_x = 0.065$ and $h_y = 0.065$. Applying the approach from Section 3, accuracy up to $e^h = 1.8e-5$ is assumed in both x and y . Thus, a compression error tolerance of $\epsilon < 1.8e-5$ is required such that error added due to compression into this does not impact simulation results. The tolerance $\epsilon = 1e-6$ is selected to allow for accumulation of error due to multiple restarts. This tolerance yields an average compression factor of $7\times$. If we use a conservative tolerance—for example $\epsilon = 1e-10$ —to mitigate the impact on the application’s results as opposed to the $\epsilon = 1e-6$ tolerance selected with the aid of our methodology, the resulting checkpoint size is $2.2\times$ smaller than the original. Our method yields a checkpoint that is $7\times$ smaller than the original. Our method provides an upper bound to aid selection of a compatible compression error tolerance. In general, selecting tolerances closer to the upper bound allows for larger compression factors.

To study the propagation of error in the simulation, 75,000 time-steps are used to reach a fully developed flow. To simulate either a fail-stop failure or exceeding a time allocation at time-step 15,000, 30,000, and 45,000, the simulation restarts from a lossy compressed checkpoint. Figure 10 plots the max-norm between the numerical solution u^h and the compressed numerical solution \tilde{u}^h . With each checkpoint there is an increase in error in the system, but the error from lossy compression and advancing the simulation from lossy state is always less than truncation error.

Between the first and second restart (time-steps 15,000–30,000), there is a reduction in the error of all state

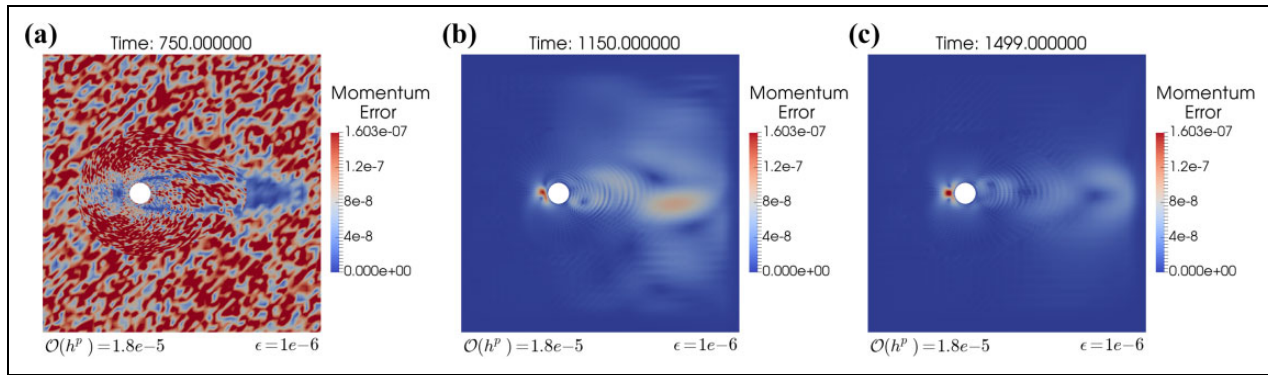


Figure 9. Propagation of momentum error in PlasComCM. a) Time-step 15000: Distribution of compression error due to lossy restart. Overset grid is visible in error. (b) Time-step 23000: Error propagates through domain in direction of flow (to the right). (c) Time-step 29980: Error accumulates in regions of low momentum, Figure 6.

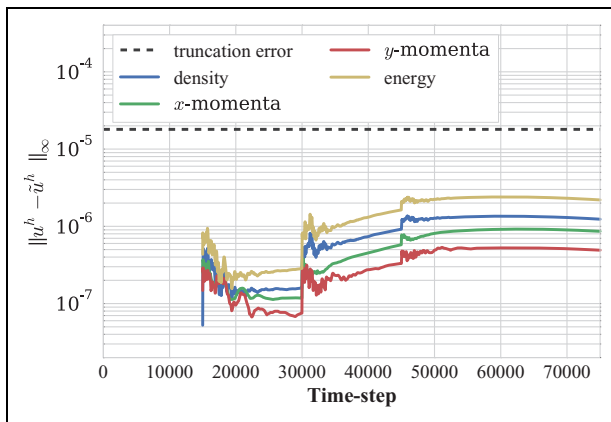


Figure 10. Max-norm between numerical solution u^h and compressed numerical solution \tilde{u}^h for PlasComCM.

variables. This is due to the selection of nonperiodic boundary conditions, which allow the error to flow out of the domain. However, between the second and third restart (time-steps 30,000–45,000), the magnitude of error increases due to concentration of error in regions of the domain with low momentum—that is, to the left of the cylindrical object. After the third restart, the simulation evolves another 30,000 time-steps in order to allow the error to accumulate. Over these time-steps, the error remains near the compression tolerance of $\epsilon = 1e-6$, and there is a slow reduction as error moves from regions of low momentum to regions of higher momentum before exiting the domain.

The restart frequency used in this problem corresponds to a system MTBF of approximately 18 min. This MTBF is much lower than the MTBF of current systems and expected exascale systems but does highlight the nature of error propagation/accumulation for this problem. If the frequency of restarting from lossy checkpoints is high, then error accumulation above the level of truncation error can occur. In this case, a smaller compression tolerance ϵ should be used minimizing the risk of exceeding the level of truncation error.

Visualizing the error, Figure 9, in the simulation highlights two key properties about this problem's handling of

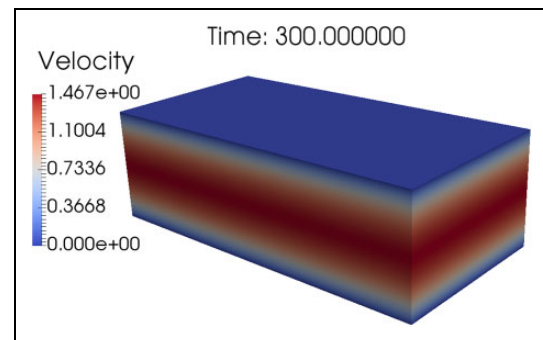


Figure 11. Magnitude of velocity after 30,000 time-steps for Nek5000.

error. First, the domain has nonperiodic boundary conditions. This allows flow that is slightly perturbed to leave the simulation as time evolves reducing the amount of error. Any error that accumulates above or below the cylindrical object is removed from the domain as its path out of the domain is unobstructed. Second, in the same momentum error plots, Figure 9, a large spike in error is observed near the leftmost part of the fixed cylindrical object. Accumulation of error at this point is due to the near-zero momentum (cf. Figure 6). With almost no momentum to move this error through the domain, it becomes concentrated and slowly increases in magnitude as time evolves. These domain-specific properties of error propagation suggest that lossy compression routines can improve by adjusting compression error tolerances to the physical properties of the domain that can accumulate or propagate error.

5.2. Nek5000

Nek5000⁸ is a spectral element code developed at Argonne National Laboratory designed to simulate a variety of problem types such as heat transfer, unsteady incompressible Navier–Stokes flow, and incompressible magnetohydrodynamics. Production runs checkpoint 0.1–2 MB of data per process using an application-specific checkpointing routine and binary file format.

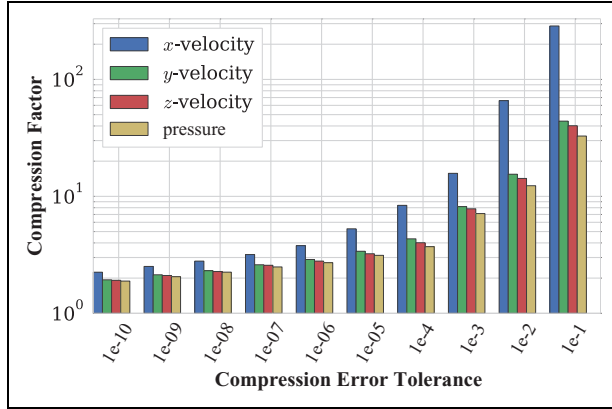


Figure 12. Smaller compression tolerances lead to higher compression factors for Nek5000.

The test problem considered in this example is a 3-D Navier–Stokes simulation of a channel flow with periodic boundary conditions. Figure 11 shows the solution of velocity at 30,000 time-steps. The simulation restarts twice during execution at time-step 1500 and time-step 11,500 (MTBF of 50 min). This test problem is run with 16 processes, each checkpointing about 1 MB of data.

Compression factors for Nek5000, shown in Figure 12, are as high as $280\times$ for the x -component of velocity with compression tolerance $\epsilon = 1e-1$. As the compression error tolerance decreases, compression factors approach $2\times$ for all variables. The discrepancy in compression factors between the x -component of velocity and the other variables is due to the x -direction of the flow. Without flow obstacles, the x -component of velocity is generally more uniform than other spatial components of the velocity. The more uniform nature allows SZ to more accurately predict values. SZ adopts curve fitting to predict future values in the array. If a section of data is easily represented with a curve fitting predictor, then compression factors are high. If the data are not easily predicted by curve fitting, SZ utilizes binary analysis on the hard-to-compress regions. However, binary analysis is less effective at reducing data size in comparison to curve fitting. This also suggests that compressors more directly designed for physical properties may yield improved compression factors.

Compression time of the Nek5000 state variables, shown in Figure 13, falls within two regimes that mirror the compression factor results. Variables that are easier to compress and exhibit large compression factors take less time than difficult-to-compress variables. Spatially smooth data are often easier to compress. Furthermore, selection of the lossy compressor can greatly influence the time to compress and compression factor (Di and Cappello, 2016; Tao et al., 2017). This highlights a need for further study into the development of specialized compressors that are tailored to certain state variables in PDEs.

The 3-D channel flow problem solves two linear systems at each time-step: one for pressure and one for velocity. The

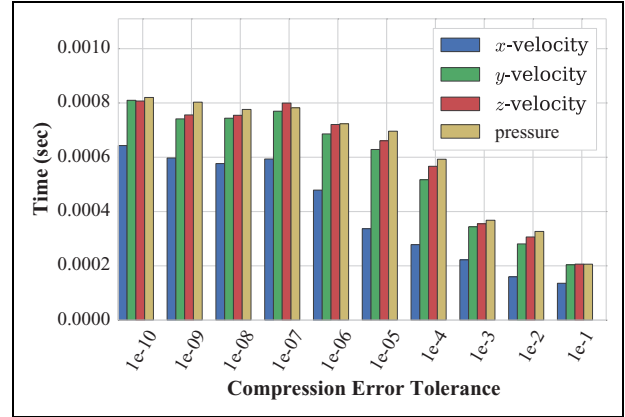


Figure 13. Time to compress (per process, single threaded) for Nek5000 increases as the error tolerance decreases. Easy to compress data compresses faster, Figure 12.

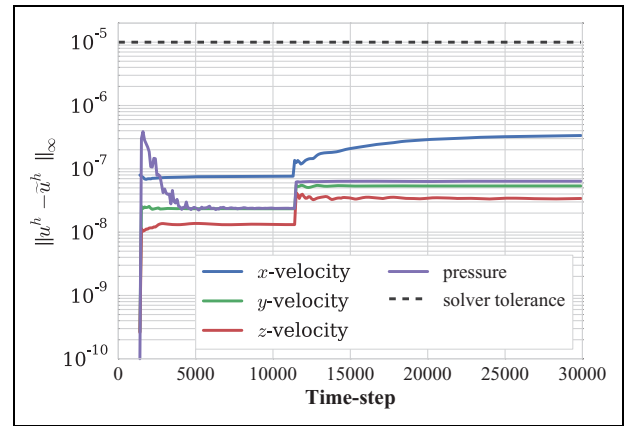


Figure 14. Max-norm between numerical solution u^h and compressed numerical solution \tilde{u}^h for pressure and velocity for Nek5000. There is no error before time-step 1500 as the simulation is not yet restarted.

linear systems for pressure and velocity are solved using the generalized minimal residual method (GMRES) to a tolerance of $e^h = 1e-5$. The accuracy to which the linear systems are solved suggests compression tolerances $\epsilon < 1e-5$ are required. Due to periodic boundary conditions that do not permit error to escape the domain, the compression tolerance is set at $\epsilon = 1e-7$, allowing for an increase in error due to multiple restarts. While using a more conservative bound of $\epsilon = 1e-10$ results in a compression factor of $2\times$ over the original, our method of selecting ϵ results in a compression factor of $2.8\times$ over the original.

Figure 14 shows the maximum error in the pressure along with the directional components of velocity between the numerical solution u^h and a compressed numerical solution \tilde{u}^h . After restarting from a lossy checkpoint, there is an initial spike in error in the time-steps immediately following the restart, but it remains below the discretization error. As time evolves, the error reduces as it migrates through the domain and approaches a steady state (due to the periodic boundary conditions). After the second restart, at time-step 11,500,

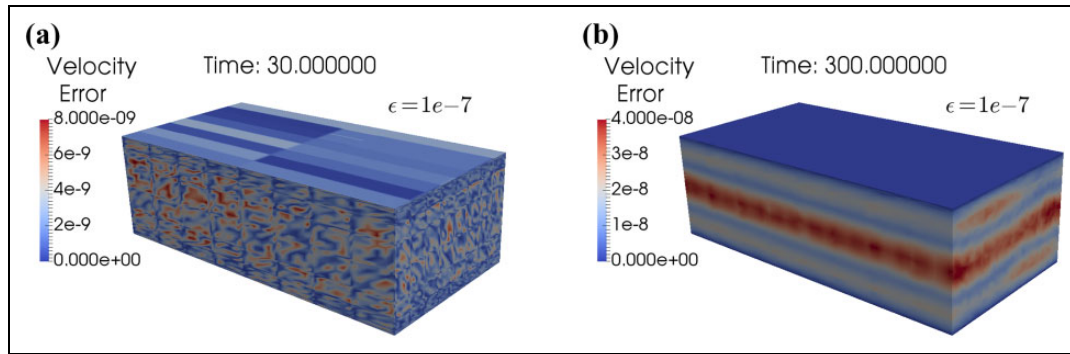


Figure 15. Propagation of velocity error in Nek5000. **(a)** Time-step 1,500: Distribution of compression error due to lossy restart. Processor boundaries are visible. **(b)** Time-step 30,000: Error in velocity magnitude for Nek5000 from Figure 11.

there is another spike in error due to restarting from lossy state. As time evolves, the error propagates though the domain but remains less than discretization error.

Figure 15 shows the spatial location of error for the velocity solution in Figure 11 at time-step 30,000. Regions of large error correspond to regions of high velocity. The initial distribution of error after a lossy restart, Figure 15(a), illustrates processor boundaries and data distribution. Even though ghost regions on other processors are needed to advance the simulation, SZ's compression algorithm only considers local data when compressing. This results in faster compression times but results in compression artifacts around processor boundaries. Compression artifacts are magnified when the per-process distribution of data is not spatially contiguous. Values that appear to be neighbors locally due to how data are stored may in fact be distant globally leading to compression artifacts and lower compression rates.

6. Modeling time to checkpoint

The previous sections show that leveraging the truncation error of HPC applications is an effective method of selecting a lossy compression error tolerance when compressing checkpoint files. Ultimately, however, lossy compression should be used for checkpointing only if it results in a more efficient time to checkpoint. To explore trade-offs for lossy compression, the time to checkpoint is modeled for an averaged size job run on a machine similar to Blue Waters. A simple model for time to checkpoint, T , is given by

$$T = c_b \cdot V + \frac{w_b \cdot V}{f}, \quad (7)$$

where c_b is the bandwidth of the compressor, V is the number of bytes being written per process, w_b is the file system bandwidth, and f is the compression factor of the compressor. For the case without lossy compression, $c_b = 0$ and $f = 1$. For lossy compression to be useful, the time to checkpoint using lossy compression, T_{lossy} , needs to be less than the time to checkpoint without compression, T_{reg} : $T_{\text{lossy}} < T_{\text{reg}}$. This simplifies to

$$f > \frac{w_b}{w_b - c_b}, \quad (8)$$

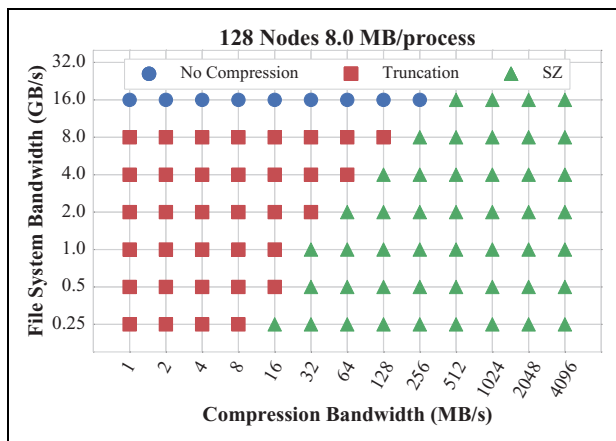


Figure 16. Fastest I/O configuration with various file systems and compression bandwidths (64-bit floating-point data set).

which is used to estimate the minimum compression factor for lossy compression to be viable. This model does not take into consideration the complex nature of the parallel I/O system. Despite this limitation, however, the model is useful to estimate when compression improves performance. A more refined I/O model (Isaila et al., 2015) that considers the parallel data exchanges in collective I/O reads/writes is parametrized for Blue Waters.

Figure 16 explores when lossy compressing checkpoint files improves performance for various combinations of compression bandwidth and file system bandwidth for a parallel job. The parallel job consists of 2048 processes on 128 nodes (1 process per core) each checkpointing 8 MB of data.⁹ Lossy compression is not pipelined with file I/O in the modeling. Two lossy compressors are modeled in Figure 16. The first lossy compressor is *Truncation* which truncates 64-bit floating-point values to 32-bit values, resulting in a 2× reduction in checkpoint size. Since this compressor performs no extra computation beyond truncating each floating-point value, this compressor's performance is limited only by the available memory bandwidth. Therefore, the compression bandwidth is set as a fixed measured constant 5.4 GB/s per core. The second lossy compressor is SZ, which models SZ-1.3. The compression factor is set at 7× and is

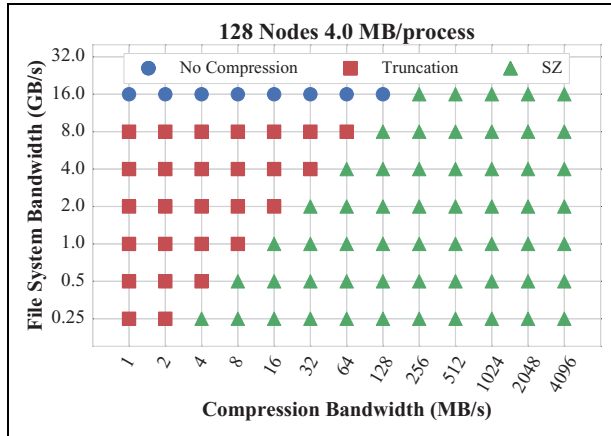


Figure 17. Fastest I/O configuration with various file systems and compression bandwidths (32-bit floating-point data set).

compatible with observed factors in both PlasComCM and Nek5000. *SZ*'s compression is more computationally intense than *Truncation*. Therefore, the compression bandwidth is a function of the checkpoint data. Easier-to-compress data compresses faster than more difficult-to-compress data. This results in variability in the observed compression bandwidth. Figure 16 scales the compression bandwidth for *SZ* from 1 MB/s to 4 GB/s.

Figure 16 shows lossy compression becomes increasingly attractive as compression bandwidth increases relative to I/O bandwidth. Practice shows effective I/O bandwidth is much less than peak (Luu et al., 2015), while compression can reach memory bandwidth. For example, PlasComCM runs of this size achieve an average aggregate file system bandwidth of around 2 GB/s on Blue Waters when checkpointing. A compression bandwidth of 64 MB/s is enough to improve the time to checkpoint. The measured compression bandwidth for PlasComCM¹⁰ is 78 MB/s. For PlasComCM, lossy compression can improve checkpointing time by $1.8\times$ compared to standard checkpointing.

If the computation is performed on 32-bit floating-point values instead of 64-bit floating-point values, the default size of the checkpoint is reduced from 8 MB/process to 4 MB/process. Moreover, this a priori reduction in data size decreases the performance of lossy compression in both compression factor and compression bandwidth. In our experiments, compressing 32-bit data sets results in compression factors that are roughly half of the compression factor for a 64-bit data set. Furthermore, compression bandwidths are two-thirds of the bandwidth of compressing 64-bit data sets. Regardless, the resulting compressed checkpoint size for a 32-bit data set is smaller than the compressed checkpoint size of the 64-bit data set. Figure 17 shows lossy compressing the 32-bit data set improves time to checkpoint. For PlasComCM, performance can be improved by $1.12\times$.

Using Amdahl's law and the more realistic performance model from Isaila et al. (2015), we compute the application speedup for various I/O fractions ranging from 1% to 90% in Figure 18. As the I/O fraction increases, the application

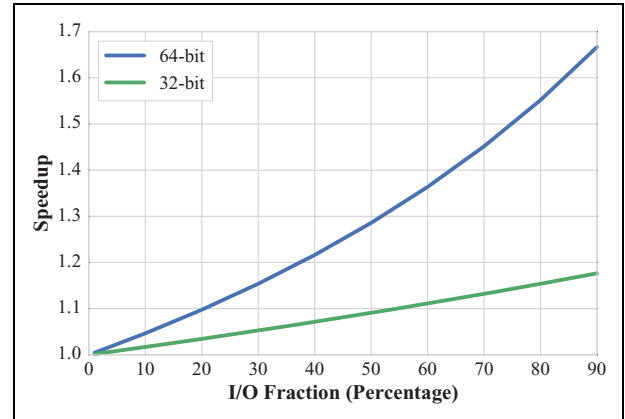


Figure 18. Application speedup due to improving the I/O with lossy compression.

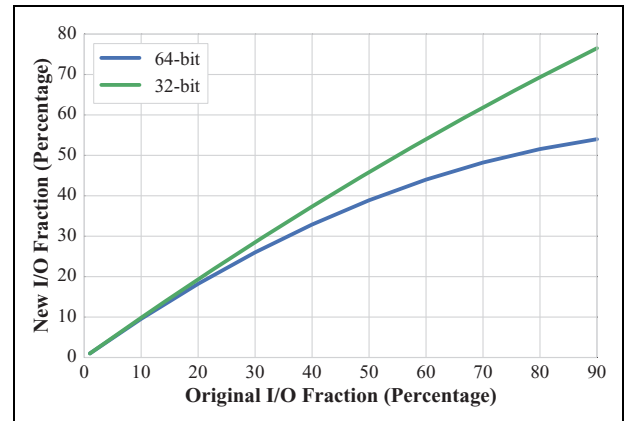


Figure 19. I/O fraction after using lossy compression.

speedup approaches the speedup obtained from using lossy compression during I/O. Improving I/O performance impacts the I/O fraction of the application. Figure 19 shows the new I/O fraction after using lossy compression. For applications that spend significant amounts of time in I/O, lossy compression is effective at reducing the I/O fraction. Moreover, as research continues to improve the performance of lossy compressors, we will see further improvement in application runtime and a reduction in the I/O fraction of the application.

7. Discussion

The previous sections explore the feasibility of setting lossy compressor error tolerances based on the numerical accuracy of the simulation. Results show that introducing compression error less than the numerical truncation error results in minimal impact on the simulation. Yet, there are several directions of development that would improve lossy checkpointing and increase its utility in practice.

7.1. Error accumulation

Error propagation after a restart and the frequency of restarts complicate the process of selecting a compression

tolerance. Further analysis on the propagation of error due to lossy compression and quantifying the compression error is needed. In addition, the impact of multiple restarts and effect on the convergence rate should be explored.

7.2. Physics-based compression

Simulations often rely on the conservation of key quantities—for example, mass, energy—require symmetries in the domain, or compute statistics on state variables. Development of compressors that are designed specifically for certain physical properties could ensure key properties are satisfied.

7.3. Adaptive compression

This article uses one global compression error tolerance for all checkpoints and variables because we test the validity of our approach and not an optimal implementation. In a production setting, using different tolerances spatially and temporally for all state variables will allow new optimizations that further reduce checkpoint size and mitigate the effect of error accumulation.

7.4. Lower precision computation

This work considers computation on double precision data. If computation is performed on lower precision, single or half precision, lossy compression can still be employed but requires more from the lossy compressor in terms of compression factor and/or compression time. Using single or half precision reduces the data set size by $2\times$ or $4\times$ compared to double precision. Lossy compressing lower-precision data sets results in smaller compression factors and smaller compression bandwidths. However, performance improvement is possible (Figure 17). Using lossy compression inside applications that use mixed-precision floating-point arithmetic is interesting future work because it allows for further refinement of the compression error tolerance based on accuracy needs at certain points in the computation.

8. Conclusion

Checkpoint restart is an integral part of long-running HPC applications. Yet, data movement is becoming a key bottleneck on current and future machines. In response, lossy compression is a method to effectively reduce the volume of data required for a checkpoint, but at the expense of adding error into the simulation. The compression error tolerance is often difficult to determine a priori. This article investigates the feasibility of using numerical truncation error as a basis for selecting the lossy compression error tolerance. First by demonstrating this use on a 1-D heat and 1-D advection equation, it is shown that error introduced through compression can have limited impact on the simulation. In addition, results for two production-level HPC applications PlacComCM and Nek5000 also highlight its

use. Results show that limiting lossy compression error to that of the discretization error allows simulations to restart from a lossy compressed checkpoint without significantly impacting the simulation. Finally, lossy compression is shown to reduce checkpoint time for compression error bounds that respect the truncation error of the application.

Declaration of Conflicting Interests

The author(s) declared no potential conflicts of interest with respect to the research, authorship, and/or publication of this article.

Funding

The author(s) disclosed receipt of the following financial support for the research, authorship, and/or publication of this article: This work was sponsored by the Air Force Office of Scientific Research under grant FA9550-12-1-0478 and part of the Blue Waters sustained-petascale computing project, which is supported by the National Science Foundation (awards OCI-0725070 and ACI-1238993) and the state of Illinois. Blue Waters is a joint effort of the University of Illinois at Urbana-Champaign and its National Center for Supercomputing Applications. This material is also based in part on work supported by the Department of Energy, National Nuclear Security Administration, under award no DE-NA0002374 and is based upon work supported by the National Science Foundation under grant no SHF-1617488.

Notes

1. <https://asc.llnl.gov/coral-info>.
2. <https://www.olcf.ornl.gov/summit/>.
3. <http://xpacc.illinois.edu/>.
4. <https://nek5000.mcs.anl.gov/>.
5. The constant c may be large. To account for this, prior knowledge collected through verification runs and scaling tests can be used to create a bound on c . In this work, a large value of c is accounted for by selecting compression error tolerances that are less than the simulation's truncation error.
6. This work sets the tolerance based on the accuracy of the local truncation error and sets pessimistic, conservative bounds to mitigate accumulation of error during the remaining time-steps.
7. <https://bitbucket.org/xpacc-dev/plascomcm>.
8. <https://github.com/Nek5000/Nek5000>.
9. Increasing the per-process data size causes the trade-off point between *SZ* and *Truncation* to shift to the right—that is, *SZ* requires a faster compression bandwidth to become the most effective scheme for a constant compression factor. If the compression factor scales with data set size, the trade-off point between *SZ* and *Truncation* is similar to that presented in Figure 16.
10. Data compressed to $\epsilon = 1e-6$ with a single threaded unoptimized SZ-1.3 using relative and absolute error bounds.

References

- Baker AH, Xu H, Dennis JM, et al. (2014) A methodology for evaluating the impact of data compression on climate simulation data. In: *Proceedings of the 23rd international symposium on high-performance parallel and distributed computing, HPDC '14*. New York, USA: ACM, pp. 203–214. ISBN 978-1-4503-2749-7. DOI: 10.1145/2600212.2600217. Available at: <http://doi.acm.org/10.1145/2600212.2600217>
- Bautista-Gomez L, Tsuboi S, Komatitsch D, et al. (2011) FTI: high performance fault tolerance interface for hybrid systems. In: *Proceedings of 2011 international conference for high performance computing, networking, storage and analysis, SC '11*. New York, USA: ACM, pp. 32:1–32:32. ISBN 978-1-4503-0771-0. DOI: 10.1145/2063384.2063427. Available at: <http://doi.acm.org/10.1145/2063384.2063427>.
- Bergman K, Borkar S, Campbell D, et al. (2008) Exascale computing study: technology challenges in achieving exascale systems. *Defense Advanced Research Projects Agency Information Processing Techniques Office (DARPA IPTO), Technical Report 15*.
- Burtscher M and Ratanaworabhan P (2007) High throughput compression of double-precision floating-point data. In: *Data compression conference, 2007, DCC '07*. pp. 293–302. DOI: 10.1109/DCC.2007.44.
- Cappello F, Geist A, Gropp B, et al. (2009) Toward exascale resilience. *International Journal of High Performance Computing Applications* 23(4): 374–388.
- Chen Z, Son SW, Hendrix W, et al. (2014) Numarck: machine learning algorithm for resiliency and checkpointing. In: *Proceedings of the international conference for high performance computing, networking, storage and analysis, SC '14*. Piscataway, NJ, USA: IEEE Press, pp. 733–744. ISBN 978-1-4799-5500-8. DOI: 10.1109/SC.2014.65. Available at: <http://dx.doi.org/10.1109/SC.2014.65>.
- Di S and Cappello F (2016) Fast error-bounded lossy HPC data compression with SZ. In: *Proceedings of the 2016 IEEE international parallel and distributed processing symposium, IPDPS '16*. Washington, DC, USA: IEEE Computer Society, pp. 730–739.
- Fischer L, Götschel S and Weiser M (2017) *Lossy Data Compression Reduces Communication Time in Hybrid Time-Parallel Integrators: Technical Report 17-25*. Berlin: ZIB.
- Ibtesham D, Arnold D, Bridges PG, et al. (2012) On the viability of compression for reducing the overheads of checkpoint/restart-based fault tolerance. In: *2012 41st international conference on parallel processing*, pp. 148–157. DOI: 10.1109/ICPP.2012.45.
- Isaila F, Balaprakash P, Wild SM, et al. (2015) Collective I/O tuning using analytical and machine learning models. In: *2015 IEEE international conference on cluster computing, CLUSTER 2015*. Chicago, IL, USA, 8–11 September 2015, pp. 128–137.
- Lakshminarasimhan S, Shah N, Ethier S, et al. (2011) *Euro-Par 2011 Parallel Processing: 17th international conference, Euro-Par 2011, Bordeaux, France, August 29–September 2, 2011, Proceedings, Part I, chapter compressing the incompressible with ISABELA: In-situ reduction of spatio-temporal data*. Berlin, Heidelberg: Springer, pp. 366–379. ISBN 978-3-642-23400-2. DOI: 10.1007/978-3-642-23400-2_34. Available at: http://dx.doi.org/10.1007/978-3-642-23400-2_34.
- Laney D, Langer S, Weber C, et al. (2013) Assessing the effects of data compression in simulations using physically motivated metrics. In: *Proceedings of the international conference on high performance computing, networking, storage and analysis, SC '13*. New York, USA: ACM, pp. 76:1–76:12. ISBN 978-1-4503-2378-9. DOI: 10.1145/2503210.2503283. Available at: <http://doi.acm.org/10.1145/2503210.2503283>.
- Lindstrom P (2014) Fixed-rate compressed floating-point arrays. *IEEE Transactions on Visualization and Computer Graphics* 20(12): 2674–2683. DOI: 10.1109/TVCG.2014.2346458.
- Lindstrom P and Isenburg M (2006) Fast and efficient compression of floating-point data. *IEEE Transactions on Visualization and Computer Graphics* 12(5): 1245–1250. DOI: 10.1109/tvcg.2006.143. Available at: <http://dx.doi.org/10.1109/tvcg.2006.143>.
- Liu N, Cope J, Carns PH, et al. (2012) On the role of burst buffers in leadership-class storage systems. In: *IEEE 28th symposium on mass storage systems and technologies, MSST 2012, April 16–20, 2012, Asilomar Conference Grounds*. CA, USA: Pacific Grove, pp. 1–11. DOI: 10.1109/MSST.2012.6232369. Available at: <http://dx.doi.org/10.1109/MSST.2012.6232369>.
- Luu H, Winslett M, Gropp W, et al. (2015) A multiplatform study of I/O behavior on petascale supercomputers. In: *Proceedings of the 24th international symposium on high-performance parallel and distributed computing, HPDC '15*. New York, USA: ACM, pp. 33–44. ISBN 978-1-4503-3550-8. DOI: 10.1145/2749246.2749269. Available at: <http://doi.acm.org/10.1145/2749246.2749269>.
- Moody A, Bronevetsky G, Mohror K, et al. (2010) Design, modeling, and evaluation of a scalable multi-level checkpointing system. In: *Proceedings of the 2010 ACM/IEEE international conference for high performance computing, networking, storage and analysis, SC '10*. Washington, DC, USA: IEEE Computer Society, pp. 1–11. ISBN 978-1-4244-7559-9. DOI: 10.1109/SC.2010.18. Available at: <http://dx.doi.org/10.1109/SC.2010.18>.
- Ni X, Islam T, Mohror K, et al. (2014) Lossy compression for checkpointing: Fallible or feasible? In: *Poster session of the 2014 ACM/IEEE international conference for high performance computing, networking, storage and analysis, SC '14*. Washington, DC, USA: IEEE Computer Society.
- Sardashti S (2015) *Using compression for energy-optimized memory hierarchies*. PhD Thesis, University of Wisconsin, Madison.
- Sasaki N, Sato K, Endo T, et al. (2015) Exploration of lossy compression for application-level checkpoint/restart. In: *Proceedings of the 2015 IEEE international parallel and distributed processing symposium, IPDPS '15*. Washington, DC, USA: IEEE Computer Society, pp. 914–922. ISBN 978-1-4799-8649-1. DOI: 10.1109/IPDPS.2015.67. Available at: <http://dx.doi.org/10.1109/IPDPS.2015.67>.

- Shalf J, Dosanjh S and Morrison J (2010) Exascale computing technology challenges. In: *High Performance Computing for Computational Science—VECPAR 2010*. Berlin, Heidelberg: Springer, pp. 1–25. Available at: <http://dl.acm.org/citation.cfm?id=1964238.1964240>
- Son SW, Chen Z, Hendrix W, et al. (2014) Data compression for the exascale computing era—survey. *Supercomputing Frontiers and Innovations* 1(2). Available at: <http://superfri.org/superfri/article/view/13>.
- Tao D, Di S, Chen Z, et al. (2017) Significantly improving lossy compression for scientific data sets based on multidimensional prediction and error-controlled quantization. In: *Proceedings of the 2017 IEEE international parallel and distributed processing symposium, IPDPS '17*. Washington, DC, USA: IEEE Computer Society.

Author biographies

Jon Calhoun is an assistant professor in the Holcombe Department of Electrical and Computer Engineering at Clemson University. He received a BS in computer science from Arkansas State University in 2012, a BS in mathematics from Arkansas State University in 2012, and a PhD in computer science from the University of Illinois at Urbana-Champaign in 2017. His research interests lie in fault tolerance and resilience for high-performance computing (HPC) systems and applications, lossy and lossless data compression, scalable numerical algorithms, power-aware computing, and approximate computing.

Franck Cappello is a senior computer scientist at Argonne National Laboratory and an adjunct associate professor in the department of computer science at University of Illinois at Urbana Champaign. He is the director of the Joint-Laboratory on Extreme Scale Computing gathering six of the leading high-performance computing institutions in the world: Argonne National Laboratory (ANL), National Center for Scientific Applications (NCSA), Inria, Barcelona Supercomputing Center (BSC), Julich Supercomputing center (JSC), and Riken AICS. He is an expert in resilience, parallel/distributed computing, and high-performance computing. Recently he started investigating lossy compression for scientific data sets to respond to the pressing needs of scientists performing large-scale simulations and experiments for significant data reduction. He is a member of the

editorial board of IEEE Transactions on Parallel and Distributed Computing and of the IEEE CCGRID steering committees. He is a fellow of the IEEE.

Luke N Olson is a professor in the Department of Computer Science at the University of Illinois at Urbana-Champaign. His PhD is in applied mathematics from the University of Colorado at Boulder in 2003 and his research interests include sparse matrix computations, multigrid methods, finite elements methods, and parallel numerical algorithms.

Marc Snir is a Michael Faiman professor in the Department of Computer Science at the University of Illinois at Urbana-Champaign. He currently pursues research in parallel computing. He received a PhD in mathematics from the Hebrew University of Jerusalem in 1979. He was director of the Mathematics and Computer Science Division at the Argonne National Laboratory from 2011 to 2016 and head of the Computer Science Department at Illinois from 2001 to 2007. Until 2001, he was a senior manager at the IBM T. J. Watson Research Center where he led the Scalable Parallel Systems research group that was responsible for major contributions to the IBM SP scalable parallel system and to the IBM Blue Gene system. He is a fellow of AAAS, ACM, and IEEE. He has Erdos number 2 and is a mathematical descendant of Jacques Salomon Hadamard. He recently won the IEEE Award for Excellence in Scalable Computing and the IEEE Seymour Cray Computer Engineering Award.

William D Gropp is a director and chief scientist of the National Center for Supercomputing Applications and holds the Thomas M. Siebel Chair in the Department of Computer Science at the University of Illinois in Urbana-Champaign. He received his PhD in Computer Science from Stanford University in 1982. He was on the faculty of the Computer Science Department of Yale University from 1982 to 1990 and from 1990 to 2007, and he was a member of the Mathematics and Computer Science Division at Argonne National Laboratory. His research interests are in parallel computing, software for scientific computing, and numerical methods for partial differential equations. He is a fellow of ACM, IEEE, and SIAM and a member of the National Academy of Engineering.